

2024

Power Generation and Water Conservation Potentials for Several Photovoltaic Configurations Installed over a Fresh Water Surface

Rana A. Kewan

Mechanical Power Engineering Department, Faculty of Engineering, Mansoura University, Mansoura, 35516, Egypt

Mohamed S. Salem

Mechanical Power Engineering Department, Faculty of Engineering, Mansoura University, Mansoura, 35516, Egypt, mohamedsameh@mans.edu.eg

Mohamed R. Elmarghany

Mechanical Power Engineering Department, Faculty of Engineering, Mansoura University, Mansoura, 35516, Egypt

Maher Bekheit

Mechanical Power Engineering Department, Faculty of Engineering, Mansoura University, Mansoura, 35516, Egypt

Gamal I. Sultan

Mechanical Power Engineering Department, Faculty of Engineering, Mansoura University, Mansoura, 35516, Egypt

Follow this and additional works at: <https://mej.researchcommons.org/home>



Part of the [Architecture Commons](#), [Engineering Commons](#), and the [Life Sciences Commons](#)

Recommended Citation

Kewan, Rana A.; Salem, Mohamed S.; Elmarghany, Mohamed R.; Bekheit, Maher; and Sultan, Gamal I. (2024) "Power Generation and Water Conservation Potentials for Several Photovoltaic Configurations Installed over a Fresh Water Surface," *Mansoura Engineering Journal*: Vol. 49 : Iss. 4 , Article 8. Available at: <https://doi.org/10.58491/2735-4202.3212>

This Original Study is brought to you for free and open access by Mansoura Engineering Journal. It has been accepted for inclusion in Mansoura Engineering Journal by an authorized editor of Mansoura Engineering Journal. For more information, please contact mej@mans.edu.eg.

ORIGINAL STUDY

Power Generation and Water Conservation Potentials for Several Photovoltaic Configurations Installed Over a Freshwater Surface

Rana A. Kewan^{a,b}, Mohamed R. Elmarghany^{a,c}, Maher Bekheit^a, Gamal I. Sultan^a, Mohamed S. Salem^{a,*}

^a Department of Mechanical Power Engineering, Faculty of Engineering, Mansoura University, Mansoura, Egypt

^b Department of Mechatronics, Faculty of Engineering, Horus University, New Damietta City, Egypt

^c Department of Mechanical Engineering, Faculty of Engineering, New Mansoura University, New Mansoura City, Egypt

Abstract

One of the challenges that face photovoltaic systems is depleting performance if their average temperature increases due to solar radiation. Floating photovoltaic (FPV) and submerged photovoltaic (SPV) systems offer a potential solution to such a problem. Another major benefit is the decrease of water evaporation by creating an artificial shadow over water. In this paper, an experimental study is presented that includes three different systems: an inclined PV by 30° over water inclined photovoltaic, an SPV, and an FPV systems, and compares their performance with that of a conventional PV system under the same operating conditions. The FPV and SPV systems exhibited average lower panel temperatures of about 8.05 °C, and 7.39 °C than the conventional PV unit. They also exhibited an increase in output power of up to 16.68% and 15.96% and an efficiency enhancement of up to 4.43% and 4.23%, respectively. The proposed systems also affected the water surface temperature, as their average temperatures significantly declined due to the panels shadow effect. The inclined photovoltaic system caused the lowest average water surface temperature. This temperature reduction led to a decrease in the water evaporation rate, with the FPV unit having the highest reduction value of about 27.5% compared with uncovered water surfaces. A specific saving rate of power and water were used to determine the most beneficial system combining the output power, and water preservation. The FPV unit displayed the highest value of specific power saving rate among all other systems, with an average value of about 27.91 W/m², as well as the greatest specific water saving rate with a value of 36%. Therefore, the FPV module proposes a viable candidate for solar generation applications over freshwater resources.

Keywords: Evaporation reduction, Floating photovoltaics, Photovoltaics, Power generation, Submerged photovoltaics

1. Introduction

The repercussions of rising energy demand, such as increased consumption of fossil fuels, global warming, and greenhouse gas emissions, necessitate the development and widespread adoption of renewable energy resources (Das et al., 2018). They are effective solutions for fulfilling energy demands and they are ecologically beneficial (Gholami et al., 2015). Solar energy is one of the

most widely used renewable energy sources. It is employed in a wide range of applications and has the potential to be a viable alternative to traditional energy resources (Ram et al., 2017). A photovoltaic (PV) system absorbs sunlight to directly generate electricity (Kumari and Geethanjali, 2018). Inverters are used to convert direct current (DC) to alternative current (AC) to be suitable for use in different applications. PV systems are characterized by their sustainability and low maintenance cost, which

Received 10 January 2024; revised 27 March 2024; accepted 14 April 2024.
Available online 23 May 2024

* Corresponding author.
E-mail address: mohamedsameh@mans.edu.eg (M.S. Salem).

<https://doi.org/10.58491/2735-4202.3212>

2735-4202/© 2024 Faculty of Engineering, Mansoura University. This is an open access article under the CC BY 4.0 license (<https://creativecommons.org/licenses/by/4.0/>).

make them profitable despite their relatively expensive installation cost.

The operating temperature is critical in the PV conversion process (Dubey et al., 2013). At an ideal operating temperature, a typical PV module converts between 5 and 20% of incident solar energy into electricity. Above the optimum temperature, more incident solar radiation is converted into heat. This leads to an increase in the PV temperature, reducing the power generation at a rate of 0.4–0.65% per degree exceeding the ideal temperature (Arpino et al., 2015). To overcome this problem, a cooling system should be designed to decrease the solar cell temperature. Active or passive cooling techniques could be used to decrease the solar cell temperature. Active cooling makes use of auxiliary cooling devices such as fans, sprinklers, and irrigators, whereas passive cooling uses natural conduction, convection, or both (Grubišić-Čabo, 2016).

Floating Photovoltaic (FPV) and Submerged Photovoltaic (SPV) systems are among the most efficient cooling techniques for PV systems. They aim to control the solar panel temperature while decreasing the free surface water evaporation rate by partially covering water bodies (Rosa-Clot et al., 2017). Water quality plays a vital role in improving system efficiency. Corrosion should be considered if the system is sited on saltwater bodies such as seas or oceans, but this problem is limited in freshwater bodies such as rivers or reservoirs. Using fresh water has several other advantages over using seawater, such as fewer algae problems, and less influence from waves and wind (Cazzaniga et al., 2018).

Several parameters influence the system performance, including solar irradiance, ambient temperature, humidity, terrain, wind speed, cooling water temperature, and module temperature. The module efficiency as well as the energy gain from the system can be enhanced by decreasing the ambient and water temperatures, as this decreases the operating temperature (Zhou et al., 2015; Liu et al., 2017). Regarding the wind speed, higher wind speed is profitable to get more heat extraction from the system, leading to higher heat transfer coefficient values and consequently improved system efficiency (Dörenkä et al., 2021; Kjeldstad et al., 2021). On the contrary, humidity has a negative effect on the system temperature and efficiency, as it diffuses the sun's rays and causes a decrease in the incident solar radiation on the PV panels (Kumar and Kumar, 2019, 2020).

Moharram et al. (2013) developed a mathematical model and an experimental setup to determine

Nomenclature:

A	Solar panel surface area [m^2]
h	Latent heat [kJ/kg]
I	Electric current [A]
m	Mass [kg]
P	Power [W]
RH	Relative humidity [%]
S	Solar radiation intensity [W/m^2]
U	Wind speed [m/s]
V	Potential difference [V]

Greek symbols

η	Efficiency
Δ	Change

Subscripts

av	Average
el	Electrical
f	Final
i	Initial
max	Maximum
oc	Open circuit
sc	Short circuit
w	Water

Abbreviations

AC	Alternative Current
DC	Direct Current
FPV	Floating Photovoltaic
GMPV	Ground-mounted Photovoltaic
IPV	Inclined Photovoltaic by 30°
PV	Photovoltaic
SPV	Submerged Photovoltaic

when to begin cooling the PV panels and how long it took to bring the panels to their normal operating temperature. It was found that the cooling rate for the solar cells was about $2^\circ\text{C}/\text{min}$ based on the concerned operating conditions. Rolla et al. (Almodfer et al., 2022) predicted the performance of a solar thermoelectric air-conditioning system (STEACS) by using hybrid artificial intelligence models. It was found that during the training stage, RVFL-JFSA predicted PV input current with R^2 values of unity for PV input current, average chamber temperature, and cooling capacity, and 0.999 for COP. During testing, R^2 values declined significantly to 0.993899, 0.999282, 0.995293, and 0.948428 for PV input current, average chamber temperature, cooling capacity, and COP. During the test stage, RVFL-AEO, RVFL-MRFO, and RVFL-SCA had R^2 values of 0.972552, 0.978477, and 0.979413 for PV input current, 0.989852, 0.999278, and 0.986937 for average chamber temperature, 0.988957, 0.982143, and 0.98311 for cooling capacity, and 0.924191, 0.833139, and 0.918452 for COP.

Mohamed *et al.* (El-Hadary *et al.*, 2023) presented a detailed computational modeling and experimental investigation for small-scale tri-generation of heat, electricity, and hydrogen and observed that by using water and air as coolants at flow rates of 40 L/h, the SPVTC-EHPC reduced the daily average PV surface temperature by 16.60% (54.46 °C) and 8.50% (59.75 °C) compared with the reference PV-EHPC system, and the daily hydrogen productivity was found to be 4.41 kg_{H2}/d for water-cooled SPVTC-EHPC (40 L/h), 4.03 kg_{H2}/d for water SPVTC-EHPC (20 L/h), 3.60 kg_{H2}/d for air-cooled SPVTC-EHPC (40 L/h), 3.24 kg_{H2}/d for air SPVTC-EHPC (20 L/h), and 3.07 kg_{H2}/d for conventional PV module EHPC. El-Agouz *et al.* (2022) considered a specific emphasis on hybridization configurations, energy performance evaluation, and economic studies of solar-MD systems. Abdelkrim *et al.* (Khelifa *et al.*, 2023) indicated numerically that the thermal efficiencies of the PVT system were 69.58, 50.02, and 34.60% using water with a flax fibers layer, pure water, and air, respectively.

Trapani *et al.* (Trapani and Millar, 2014) showed that the FPV system improved the electrical yield by 5% on average. Choi *et al.* (Choi, 2014) verified that the efficiency of the FPV system was superior by over 11% compared with the conventional one under the same operating conditions. Mittal *et al.* (2018) estimated that the yearly performance ratio and annual capacity utilization factor for a 1 MW SPV unit were about 79.52% and 19.11%, respectively. As for the comparable 1 MW FPV unit, those values were about 81.49% and 19.58%, respectively.

Liu *et al.* (2017) utilizing a finite element model, found a 3.5 °C difference in operating temperature between FPV cells and terrestrial cells. Also, an increase in FPV system efficiency of 1.58–2.00% was found compared with conventional PV systems. Liu *et al.* (2018) experimentally investigated FPV systems installed on inland freshwater reservoirs and observed that the module's temperature was generally 5–10 °C lower than similar modules mounted on rooftop environments.

Mehrotra *et al.* (2014) studied an SPV system and found a maximum increase of about 17.8% in the electrical efficiency at water depth = 1 cm. Kumar *et al.* (2020), using an experimental setup, observed that the energy efficiency of an SPV was 3.07% and 43.65% higher than that of an FPV and ground-mounted photovoltaic (GMPV) installations, respectively. It was also found that the SPV consumed 32.74% less energy than the GMPV and the FPV due to lower incoming solar radiation and lower ambient temperatures. In addition, studies have indicated that at 725 W/m² of solar energy, the

electrical efficiency without immersion was around 14.24%, while the panel efficiency at 10, 20, 30, and 40 mm immersion depths was around 15.02, 15.54, 14.58, and 13.95%, respectively (Sivakumar *et al.*, 2021).

Bontempo Scavo *et al.* (Bontempo Scavo *et al.*, 2021) developed a numerical evaporative model and found that installing the FPV on 30% of a basin area reduced evaporation by roughly 18%. Al-Widyan *et al.* (2021) estimated that a 50% basin coverage could save about 54.5% evaporations, while a 30% coverage could save 31.2% in comparison with uncovered basins. Agrawal *et al.* (2022) used a simulation model to assess the FPV power generation technical potential. The authors estimated an annual evaporation reduction of 1395 m³/MWp.

As can be seen, though several researchers investigated FPV and SPV systems performance, a limited number paid attention to the accompanying reduction in evaporation rate. In the freshwater scarcity crisis that the world is currently facing, this could be an additional benefit that should be explored more thoroughly. This paper presents an experimental setup that includes three different photovoltaic systems: FPV, SPV, and inclined photovoltaic (IPV) (inclined photovoltaic panel by 30° over water) and compares their performance with a conventional PV module (inclined by 30° over ground) under the same operating conditions. Furthermore, the effect of each configuration on the water evaporation rate reduction rate by shade is investigated.

2. Materials and methods

2.1. Instrumentation

The solar irradiance was measured using a solar power meter (TM-206) with uncertainty ±10 W/m². The solar panels surface temperatures were measured using thermocouples mounted on their top surfaces (Type-J) with an uncertainty of about ±1 °C. The same type of thermocouples located in the middle of the water basins was used to measure the water temperatures. All temperatures obtained were recorded using a data logger (GRAPHTEC midi LOGGER GL240). Wind velocity (U) and relative humidity (RH) were measured with (LUTRON LM-8102), with uncertainties ±3% and ±4 %RH, respectively. The potential and current readings of the photovoltaic panels were measured by multi-meters (UNI) with uncertainty ±0.5% in volt, and ±0.5% in current. The device should be connected in parallel to the system's electrical circuit to get the potential voltages, while connected in series to get

the current readings. The electrical circuit of the system is shown in Fig. 1.

2.2. Experimental procedure

The experiments were conducted on the roof of the Faculty of Engineering, Mansoura University which has latitude and longitude coordinates of $31^{\circ}02'10''$ N and $31^{\circ}22'50''$ E, respectively at an elevation of about 15 m above sea level. The main reason for choosing this location was the availability of a level roof with a suitable floor area devoid of any direct or indirect impact from natural or artificial shadows, as well as the availability of laboratory equipment as a data gathering center.

The research goal was to assess the performance of four different solar systems in the presence of cooling water and determine the optimum system in

terms of energy output, efficiency, and ability to reduce the water evaporation rate by draping the solar panel over a water basin and providing constant shade.

The four configurations investigated in the study are (a) An SPV system at water depth = 3 cm; (b) an FPV system; (c) an IPV system inclined by 30° over the water basin; and (d) a conventional PV system, which served as a reference panel and was installed outside the basins, away from the effects of water, as shown in Fig. 2. The solar panels in the FPV and SPV systems are in direct contact with water, whereas the solar panel in the IPV system is never in direct contact, only casting a shadow over the water surface. Detailed schema for our PV modules configurations is shown in Fig. 3.

All the experiments were carried out in October, and all readings were taken almost from 10 AM to

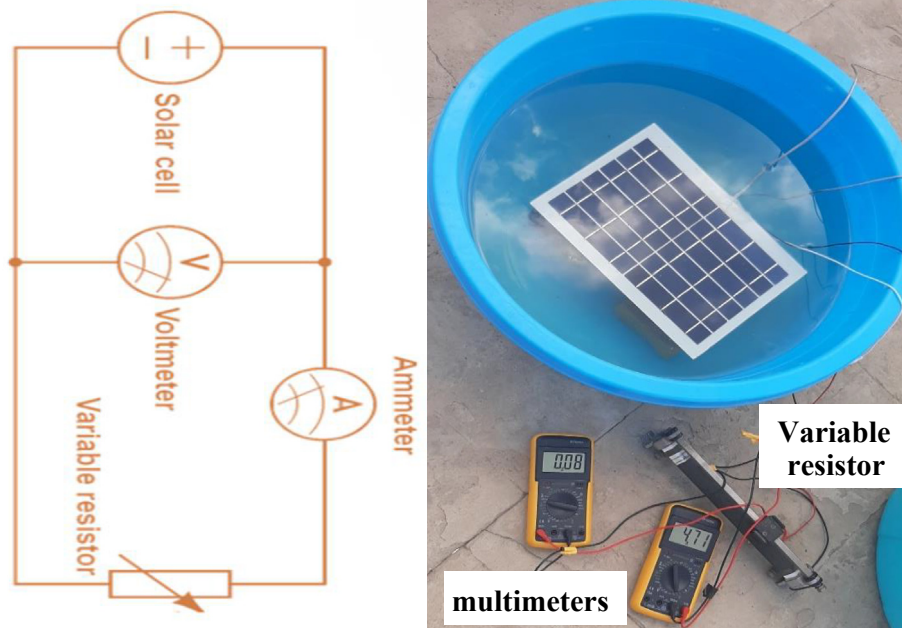


Fig. 1. Schematic diagram and actual photo of the photovoltaic system electric circuit.

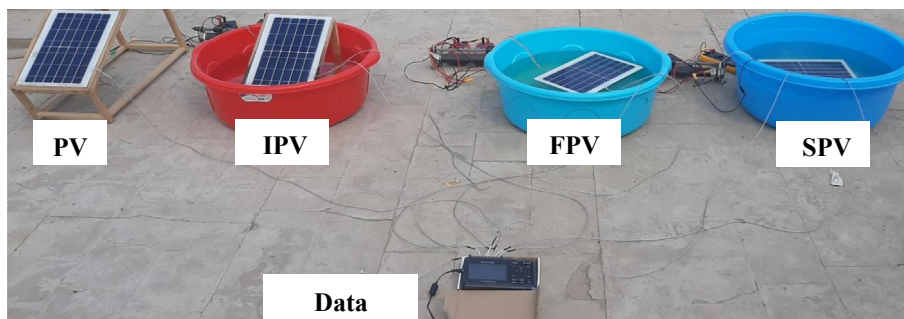


Fig. 2. The four investigated configurations (photovoltaic, inclined photovoltaic, floating photovoltaic, and submerged photovoltaic).

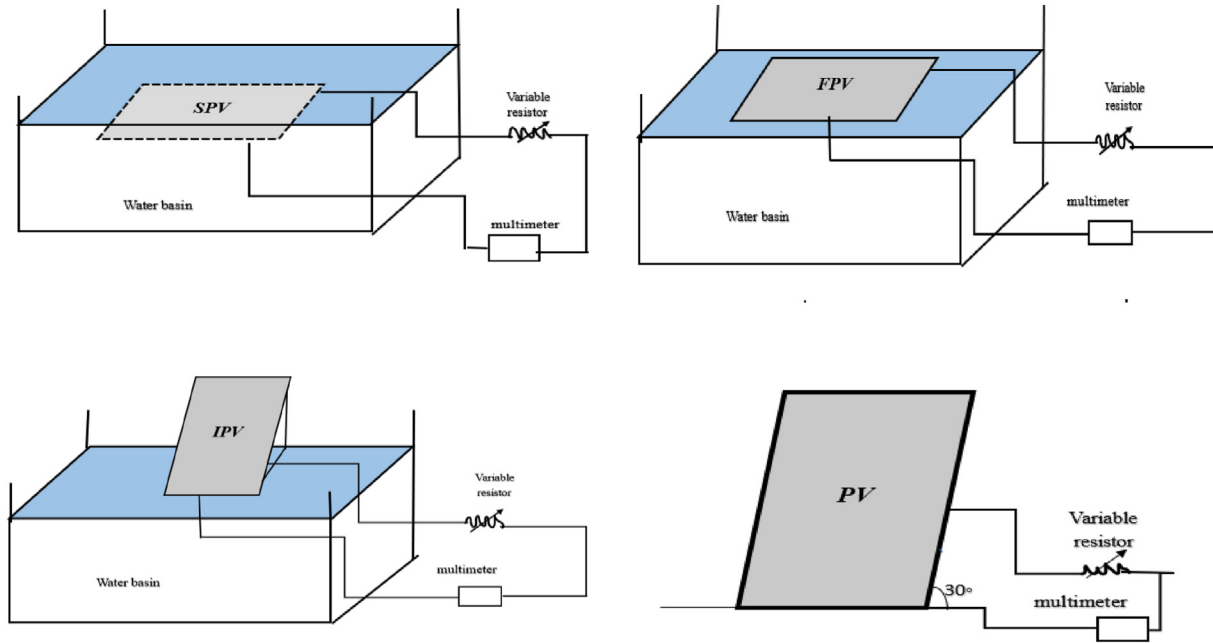


Fig. 3. Detailed schema graph for the modules' configurations.

2 PM. Four identical solar panels were used in the investigation. Their electrical and physical characteristics are shown in Table 1.

The four configurations' voltages and currents were measured with the help of a variable resistor. The short circuit current (I_{sc}) which is the current flowing through the circuit at no-load (at $V = 0$), was measured. Also, the open circuit voltage (V_{oc}) which is the maximum voltage generated by the solar cell at $I = 0$ was measured. Then, the data were recorded, tabulated, and used to create the $P - V$ and $I - V$ characteristic curves for each configuration under the same environmental and operating conditions. The power generated (P) by the solar panel could be calculated by:

$$P = I V \quad (1)$$

The solar cell efficiency can be calculated as follows (Friel et al., 2019)

Table 1. Electrical and physical characteristics of the used photovoltaic modules.

Electrical and physical characteristics	
Cell type	Monocrystalline silicon
No. of cells per panel	12
Glass Dim. [mm]	244 × 344
Cell Dim. [mm]	30 × 156
Volt [V]	6
Current [A]	1.66
Power [W]	10

$$\eta_{el} = \frac{P}{S * A_{pv}} \times 100\% \quad (2)$$

Where η_{el} is the electrical efficiency (%), P [W] is the power generated by the PV module, S [W/m^2] is the solar radiation intensity, and A_{pv} [m^2] is the front surface area of the PV module exposed to the sun rays.

The data were collected under various conditions in terms of solar radiation intensity, wind speed (U), relative humidity (RH), and ambient temperature. The data was used to determine the real gain in solar cell efficiency, as well as the computation for panel temperature decrease.

Additionally, the proposed configurations (i.e., IPV, FPV, and SPV modules) were put in water basins with similar surface areas. At the beginning of each experiment, each basin was filled with exactly 30 kg of water. After the experiment ended, the remaining water was weighed again to determine the weight loss by evaporation. The rate of water evaporation was determined at every case to detect the effect of the artificial shadows in saving water. Evaporation rate from an open basin was also compared with that from basins partially covered with panels to determine the system with the ability to minimize water evaporation rate.

To evaluate the proposed configurations' total performance, a specific saving rate of power and water was estimated. They are used to determine the power generated and the water evaporation

reduction rate per unit area of the PV panel as a result of using a certain configuration. The specific water-saving rate and the specific power-saving rate could be calculated from the following equations:

$$\text{Specific water saving rate} = \frac{\Delta m_{\text{saving}}^0}{A_{\text{pv}}} \quad (3)$$

$$\text{Specific power saving rate} = \frac{P_{\text{av}}}{A_{\text{pv}}} \quad (4)$$

Where $\Delta m_{\text{saving}}^0$ [kg/s] is the evaporation rate reduction.

3. Results and discussion

3.1. Temperature distribution

The surface temperatures of all the investigated panel configurations as well as the ambient temperature were recorded throughout the experiments using J-type thermocouples connected to a data logger. The temperatures were recorded every minute from 10 AM to 2 PM for several days. Two examples of the recorded temperature profiles are shown in Fig. 4.

Fig. 4a shows that the average surface temperatures of the FPV and SPV modules were 8.054 °C and 7.391 °C lower than that of the PV module respectively, which is significantly lower. This proves the hypothesis that using water as a passive cooling medium is effective in lowering the module temperature, thus allowing for better performance. However, the SPV module temperature profile exhibited the least fluctuation in temperature values. This may be due to the fact that the complete submergence in water shields the module from the wind effects.

On the other hand, the temperature profiles of the IPV and PV modules were almost identical. The average surface temperature of the IPV module was merely 2.082 °C higher than that of the reference PV module. This is expected as the water plays no role in cooling the IPV configuration. On the contrary, the slight increase in temperature may be due to a higher solar radiation reflection rate from the water than the ground.

Fig. 4b temperature profiles have the same trend as the average surface temperatures of the FPV and SPV modules were reduced by 7.339 °C and 7.828 °C, respectively, than that of the reference PV, whereas the IPV module had a 1.758 °C higher average surface temperature compared with the PV module. In general, FPV and SPV modules proved to have the lowest average temperatures throughout the experiments. This is very beneficial for the module's performance and efficiency.

3.2. $I - V$ and $P - V$ performance curves

The FPV, SPV, IPV, and PV configurations' electric outputs were measured at various environmental conditions such as solar radiation intensity, ambient temperature, wind speed, and relative humidity. This was done to check the systems' performance stability and effectiveness under the ever-changing weather. The measured outputs (open-circuit voltage (V_{oc}) and the short circuit current (I_{sc})) were then used to create $I - V$ and $P - V$. The characterization curves at four different environmental conditions are presented in Figs. 5–8.

As can be seen from Figs. 5a:7a, for all the investigated modules, V_{oc} and I_{sc} values increased with the increase of the solar radiation intensity. Moreover, at the same solar radiation intensity, V_{oc} values for the FPV and SPV modules were slightly higher

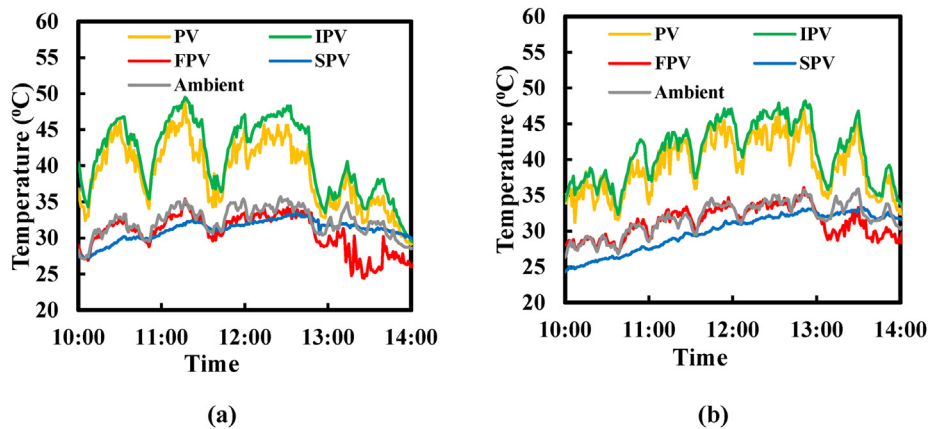


Fig. 4. Photovoltaic module temperature profiles recorded during the testing days.

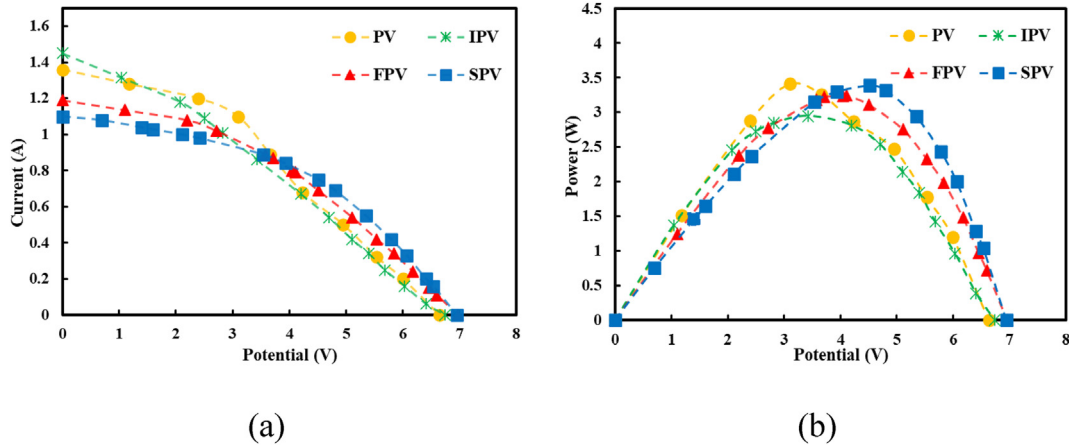


Fig. 5. (a) I–V, and (b) P–V characterization curves of the four proposed modules at $S = 697 \text{ W/m}^2$, $RH = 43.3\%$, and $U = 9.5 \text{ km/h}$.

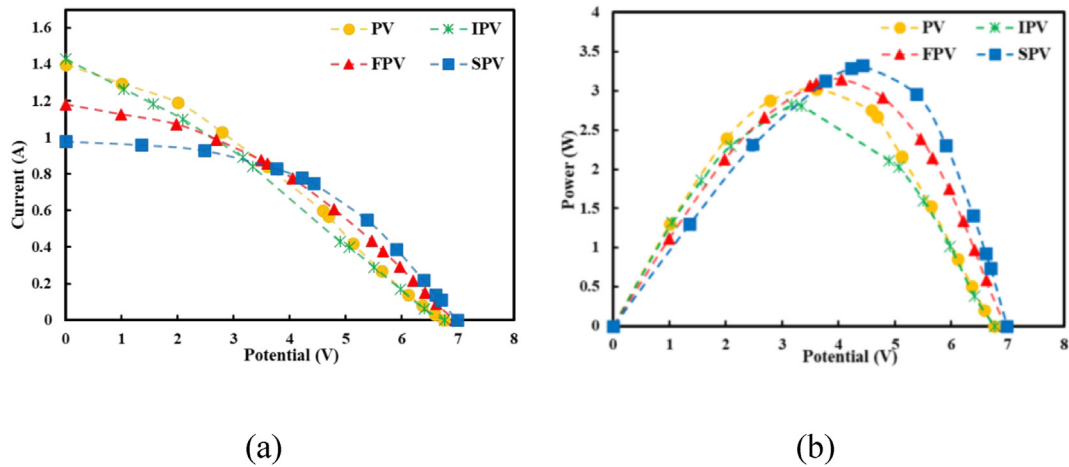


Fig. 6. (a) I–V, and (b) P–V characterization curves of the four proposed modules at $S = 655 \text{ W/m}^2$, $RH = 44.5\%$, and $U = 2.6 \text{ km/h}$.

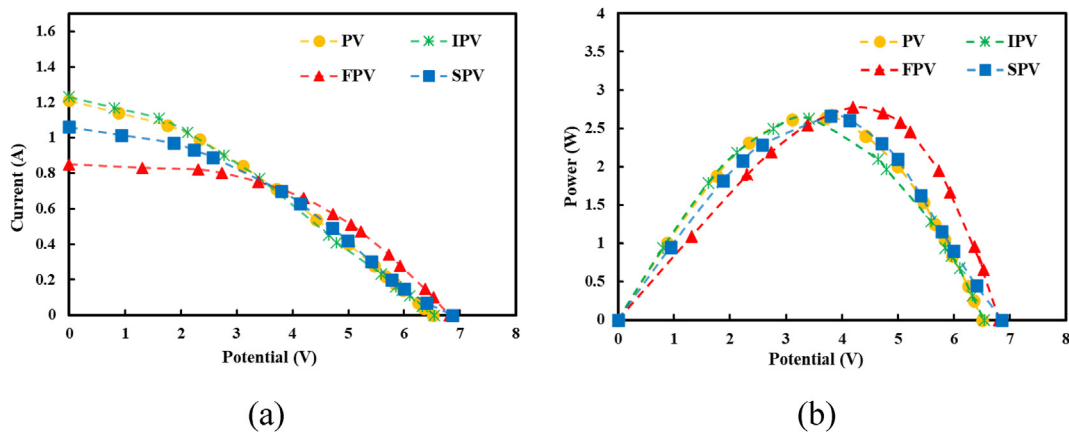


Fig. 7. (a) I–V, and (b) P–V characterization curves of the four proposed modules at $S = 585 \text{ W/m}^2$, $RH = 35\%$, and $U = 4 \text{ km/h}$.

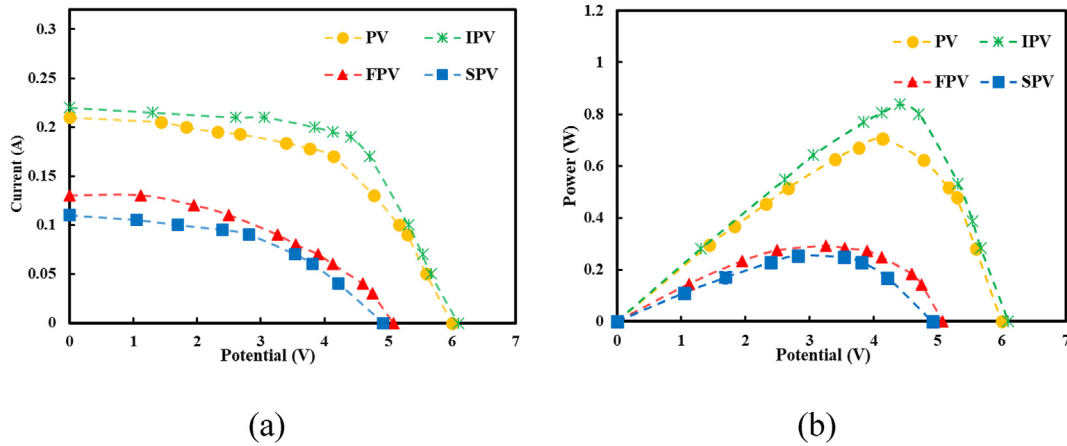


Fig. 8. (a) I - V , and (b) P - V characterization curves of the four proposed modules at $S = 95 \text{ W/m}^2$, $RH = 51.6\%$, and $U = 3.8 \text{ km/h}$.

than those of the PV and IPV modules. On the contrary, the FPV and SPV modules exhibited lower I_{sc} values than PV and IPV modules under the same environmental conditions, which agrees with the results of Azmi et al. (2013).

It is evident from Figs. 5b:7b that the power generated by FPV and SPV systems was higher than that of PV and IPV systems under the same environmental conditions. This proves that the existence of water has a positive impact on the performance of solar modules under high solar radiation intensity. This is because the basin water acts as a passive cooling system, as it extracts the excess heat from the photovoltaic panel and consequently reduces the panel operating temperature, as previously shown in Fig. 4. This can be further explored in Table 2, where the average output power and

efficiency values for the four modules were calculated at different environmental conditions.

In Table 2, the conventional PV module was taken as a reference and all the changes in output and efficiency were calculated for each of the other configurations relative to this reference. As can be seen from the table, a significant increment in the average power output of the photovoltaic panels as well as the module efficiency was noticed with the increase of the solar radiation intensity. This is expected, as the radiation intensity is the main parameter affecting the PV output.

It can be seen from the table that at relatively high radiation, the average output and efficiency of the FPV and SPV modules were higher than those of the PV and IPV modules, as previously discussed. For instance, at a solar radiation intensity of 655 W/m^2 ,

Table 2. Comparison of average power and efficiency, and percentage power and efficiency increase of floating photovoltaic, submerged photovoltaic, inclined photovoltaic, and photovoltaic modules.

Conditions	Module	Power		Efficiency	
		$P_{av.}$ [W]	Change [%]	$\eta_{av.}$ [%]	Change [%]
$S = 697 \text{ W/m}^2$, $RH = 43.3\%$, $U = 9.5 \text{ km/h}$.	PV	1.9386	—	4.21	—
	IPV	1.7460	-9.94	3.79	-9.98
	FPV	2.0414	+5.3	4.43	+5.23
	SPV	1.9505	+0.61	4.23	+0.48
$S = 655 \text{ W/m}^2$, $RH = 44.5\%$, $U = 2.6 \text{ km/h}$.	PV	1.5585	—	3.6	—
	IPV	1.5196	-2.5	3.51	-2.5
	FPV	1.8185	+16.68	4.2	+16.67
	SPV	1.8073	+15.96	4.17	+15.83
$S = 585 \text{ W/m}^2$, $RH = 35\%$, $U = 4 \text{ km/h}$.	PV	1.4287	—	3.69	—
	IPV	1.2951	-9.35	3.35	-9.21
	FPV	1.6736	+17.14	4.33	+17.34
	SPV	1.4945	+4.61	3.87	+4.88
$S = 95 \text{ W/m}^2$, $RH = 51.6\%$, $U = 3.8 \text{ km/h}$.	PV	0.4250	—	6.77	—
	IPV	0.4907	+15.46	7.81	+15.36
	FPV	0.1890	-55.53	3.0	-55.69
	SPV	0.1564	-63.2	2.49	-63.22

the average power produced by the FPV module increased by 16.68% relative to the PV module, while the SPV output improved by 15.96%. As for the average efficiency, the FPV module exhibited an increase of about 16.67%, while the SPV module displayed a 15.83% increase. This highlights the importance of using water as a passive cooling agent.

It also could be noticed that at the same radiation intensity, both the average output power and efficiency of the PV module increased by about 2.5% compared with the IPV module. This could be explained by the increase in the operating temperature of IPV module due to the slight increase in reflection rate from water than the ground, as previously discussed, which has a negative influence on the electrical efficiency and output power produced.

As for the comparison between the FPV and the SPV systems, it was found that the power output and efficiency from the former were slightly greater than the latter. This is mostly due to the decrease in solar irradiation reaching the SPV panel as a result of spectral shifts and light refraction in the water surface layer. The same previous trend could be observed at solar radiation intensities of 697 and 585 W/m^2 .

However, it was interesting to notice that on a cloudy day, where the average solar radiation intensity was measured at about 95 W/m^2 , the former trend was changed. As illustrated in Fig. 8a, both V_{oc} and I_{sc} of the PV and IPV modules held higher values than those of the FPV and SPV modules.

Fig. 8b shows that unlike at high radiation values, the PV and IPV modules produced significantly more power output than the FPV and SPV ones. In terms of power generated, the FPV module output decreased by 55.53% compared with the PV module, while the SPV module output diminished by 63.2%. This could be due to the fact that the PV and IPV

modules are inclined at an optimum angle (30°). Thus, they could efficiently make use of both direct and reflected solar radiation. This is not the case for the FPV and SPV modules, as they rely mainly on direct solar radiation because of their horizontal positioning. The cooling effect here is not as important, because the average module temperature is naturally low due to low radiation.

In Sivakumar et al. (2021), the SPV efficiency was 0.34% higher than the efficiency of conventional PV at a water depth of 3 cm, but in the present study, the SPV efficiency was 0.57% higher than the PV efficiency at the same depth. In Al-Widyan et al. (2021), the output of the FPV module increased by 5.33% as compared with the PV module, whereas in the current study, it increased by 16.68%.

3.3. Evaporation reduction

The other major advantage of placing photovoltaic systems over freshwater surfaces is to help reduce the amount of water evaporated by decreasing the area directly exposed to the sun. They also may provide shade for marine life.

The average temperature of each basin throughout the experiments was recorded, to obtain the temperature profiles of each case. Two sample results are shown in Fig. 9. As can be seen from the figures, the water temperature profiles under FPV and SPV configurations are almost identical. In Fig. 9a, the average temperatures with FPV and SPV are 30.859 $^\circ C$ and 30.394 $^\circ C$, respectively, whereas in Fig. 9b they are 29.656 $^\circ C$ and 29.479 $^\circ C$, respectively. This is expected as the two modules cover the same area of water. However, the IPV module exhibited the lowest water temperature profile with average temperatures of 29.08 $^\circ C$ and 28.213 $^\circ C$, respectively. This is even though the inclination angle decreases the shaded area. This is because the

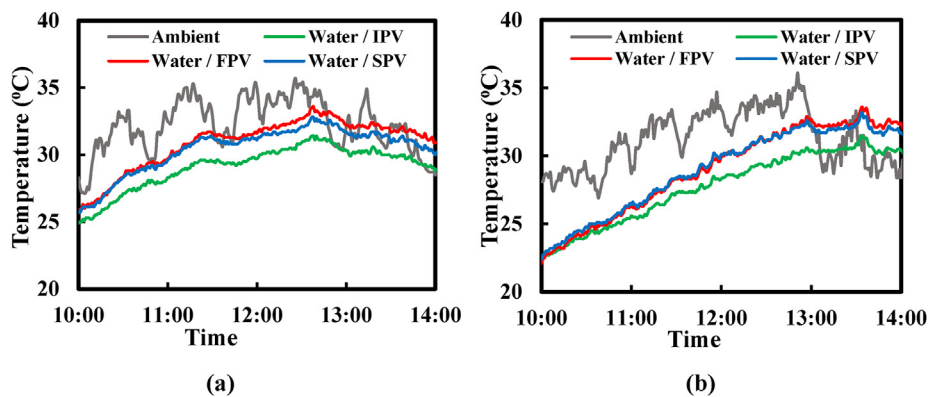


Fig. 9. Water temperature profiles for each configuration throughout the experiments.

Table 3. Water evaporation reduction rate for the inclined photovoltaic, floating photovoltaic, submerged photovoltaic modules.

Module	$m_{w, i}$ [kg]	$m_{w, f}$ [kg]	Δm [kg]	Δm_{saving} [kg/h]	Δm^o [kg/h]	Evaporation reduction rate
No-covering		20	10	—	2.5	—
IPV	30	22.25	7.75	0.625	1.9375	22.5%
FPV		22.75	7.25	0.6875	1.8125	27.5%
SPV		22.25	7.75	0.0625	1.9375	22.5%

water is not used as a cooling medium for the IPV module, thus no excess heat is added to the water body from the PV module.

As mentioned before, the amount of water in each basin was weighed before and after each experiment, to determine the average decrease in weight due to evaporation. The average results are shown in Table 3. As can be seen from the table, the highest evaporation rate was in the case of the basin with no covering, which was taken as a reference. An average of 33.33% of the water evaporated during the experiments time (4 h).

The IPV and SPV modules exhibited almost the same ability to reduce water evaporation rate by about 22.5% compared with the no-covering case. However, The FPV module proved to have the highest water evaporation reduction potential with a reduction rate of about 27.5%. This is an acceptable result as the FPV module shades a bigger surface area than the IPV module. On the other hand, as it's submerged, the SPV module doesn't prevent the upmost surface layer of water from direct exposure to solar radiation.

To indicate inputs, constraints, and weather, operative, and design variables of the experiment, a flow chart is shown in Fig. 10.

3.4. Saving estimation

As previously mentioned, to evaluate the performance of each module, the specific power and

water-saving rates were calculated that combine the module's ability to produce electricity with its effect on the evaporation rate. The specific power saving rates for three different experiments ($S = 697, 655, 585 \text{ W/m}^2$) were calculated and the results are shown in Fig. 11.

As Fig. 11 shows, the FPV module proved to have the highest specific power saving rate for all the cases, as it exhibited relatively high power output, along with a high evaporation reduction rate. On the other hand, the SPV and IPV modules maintained a relatively close specific power saving rate value in all the cases, as they exhibited similar ability to produce close power outputs. The FPV had the highest average specific power saving rate value of about 27.91 W/m^2 .

According to specific water saving rate, the FPV module had the best one with a nearly value of $8.19 \text{ kg/m}^2\text{hr}$. On the contrary, the SPV and IPV modules maintained at a relatively close specific water saving rate value of approximately $7.45 \text{ kg/m}^2\text{hr}$.

The averages prices of water and electricity announced by the holding company for water and waste water and the ministry of electricity and renewable energy by year 2024 are 2.07 L.E./m^3 , and 1.13 L.E./kW . So, according to the current study the saving costs are as follows in Tables 4 and 5.

4. Uncertainty analysis

In this study, the measured experimental parameters are the potential voltages and current readings

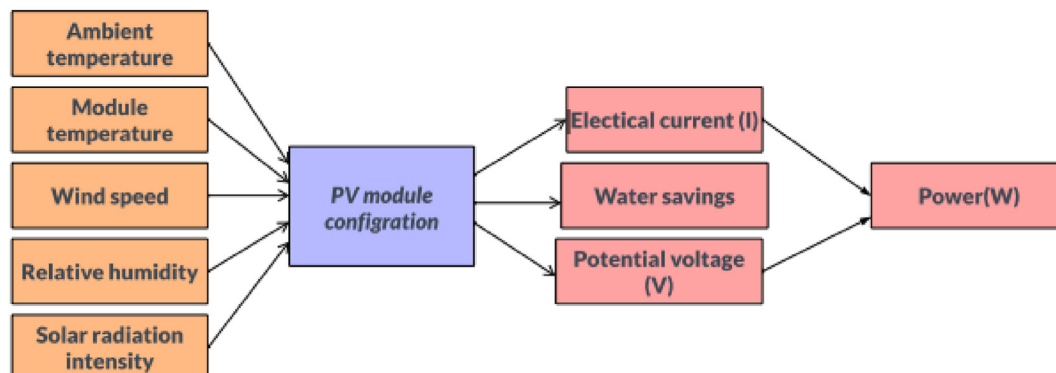


Fig. 10. A flow chart of the conducted calculations.

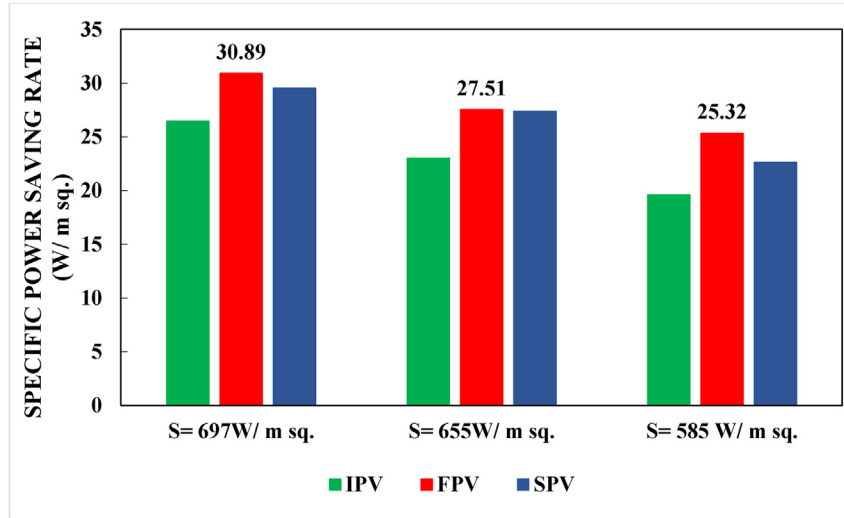


Fig. 11. Specific power saving rate for inclined photovoltaic, floating photovoltaic, and submerged photovoltaic modules at different solar radiations.

Table 4. Saving cost for evaporation reduction.

Module	$\Delta m_{\text{saving}} (m^3)$	Saving cost (L.E.)
IPV	2.5×10^{-3}	0.005175
FPV	2.75×10^{-3}	0.0056925
SPV	2.5×10^{-3}	0.005175

by using eight UNI-T devices with uncertainty $\pm 0.5\%$ in volt and current, and the solar radiation intensity via a solar power meter (TM-206) with uncertainty $\pm 10 W/m^2$. The following formula is used to assess the uncertainty of the evaluated parameters (Kandil et al., 2023).

$$\omega(x) = \sqrt{\left(\sum_{i=1}^N \left(\frac{\partial X}{\partial X_i} \right)^2 \omega_{x_i}^2 \right)} \quad (5)$$

Table 5. Saving cost for power produced.

Conditions	Module	Power	Saving cost (L.E.)
		$\overline{P_{av.}} [W]$	
S = 697 W/m ² , RH = 43.3%, U = 9.5 km/h.	PV	1.9386	0.00219
	IPV	1.7460	0.00197
	FPV	2.0414	0.00231
	SPV	1.9505	0.0022
	PV	1.5585	0.00176
S = 655 W/m ² , RH = 44.5%, U = 2.6 km/h.	IPV	1.5196	0.00172
	FPV	1.8185	0.00205
	SPV	1.8073	0.00204
	PV	1.4287	0.00161
	S = 585 W/m ² , RH = 35%, U = 4 km/h.	IPV	1.2951
FPV		1.6736	0.00189
SPV		1.4945	0.00169

where $\omega(x)$ represents the required uncertainty of dependent parameter X, and ω_{x_i} is the uncertainty of other independent parameters.

For the uncertainty analysis, Eq. 5 is used to evaluate the uncertainty in calculating the output power, and the corresponding efficiency. Small values of the measured parameters are used to maximize the error. The chosen values were a current reading of 0.03 A, with a potential reading of about 6.59 V under a solar radiation intensity of 655 W/m².

The uncertainty in the output power was found to be $\pm 0.707\%$, while the uncertainty in the efficiency was found to be about $\pm 1.638\%$.

5. Conclusions

This study covers the two main positive impacts of laying PV panels over freshwater, namely the improved panel efficiency due to passive cooling of the PV panel from the water beneath and the avoidance of water evaporation caused by generating an artificial shadow over the water. With a suitable design, it may be possible to enhance total energy generation while decreasing water evaporation and therefore minimizing land stress.

In the current study, three main configurations were experimentally investigated under the same environmental conditions and compared with the performance of a conventional PV system. The three systems are an inclined IPV system, a floating FPV system, and a submerged SPV system. The systems were studied under different environmental effects, and their output and characteristics were recorded.

As for the average panel temperature, the FPV and SPV exhibited significantly lower values compared with the conventional PV panel and the

IPV system, due to better cooling. The average recorded temperatures for the FPV and SPV systems were approximately 8.054 °C and 7.391 °C lower than the PV unit.

This is reflected in the output power and efficiency, where at high solar intensity values, the FPV and SPV systems exhibited a high increase in power of 16.68% and 15.96% over the conventional PV unit under the same conditions.

As for the water surface temperature, the IPV, FPV and SPV systems proved the ability to reduce the average temperature through creating a shadow over the water. However, the IPV exhibited the highest ability to reduce water temperature as it doesn't use the water as a cooling medium.

The three systems placements also led to a significant reduction in the water evaporation rate compared with uncovered water surfaces. However, the FPV system exhibited the highest ability with a reduction rate of about 27.5%.

Finally, a utilization factor (UF) was calculated to combine the two main benefits of the proposed systems. The FPV configuration exhibited the highest values at all the investigated cases, with an average UF of about 10.23.

Therefore, the FPV module proved to be the most suitable configuration to achieve satisfying power output and high evaporation reduction rate within the investigated cases.

During the experiment, we encountered some challenges, such as the inability to investigate the influence of water waves movement and the effect of tidal forces on the efficiency of solar panels and the amount of power generated. Furthermore, the experiment's inability to study the effect of terrains and humidity on the power generated by the panels, as well as the small size of the water body used, is a limitation of the experiment.

Therefore, in future work, we recommend addressing such variables and studying their impact on the overall efficiency of the system and power produced.

Ethics information

The authors declare that no breach of scientific ethical behavior was breached during this study.

Funding

No external Funding was used for this research.

Author contributions

The authors confirm contribution to the paper as follows: Study conception and design: Salem and

Elmarghany; data collection: Kewan and Salem; analysis and interpretation of results: Bekheit, Elmarghany, and Sultan; draft manuscript preparation: Kewan; draft review: Bekheit and Sultan. All authors approved the final version of the manuscript.

Conflicts of interest

There are no conflicts of interest.

Acknowledgment

All the coauthors would like to express their deepest gratitude our mentor, Prof. Gamal I. Sultan, who recently passed away. May allah rest his soul.

References

- Agrawal, K.K., Jha, S.K., Mittal, R.K., Vashishtha, S., 2022. Assessment of floating solar PV (FSPV) potential and water conservation: Case study on Rajghat Dam in Uttar Pradesh, India. *Energy Sustain. Dev.* 66, 287–295.
- Almodfer, R., Zayed, M.E., Elaziz, M.A., Aboelmaaref, M.M., Mudhsh, M., Elsheikh, A.H., 2022. Modeling of a solar-powered thermoelectric air-conditioning system using a random vector functional link network integrated with jellyfish search algorithm. *Case Stud. Therm. Eng.* 31, 101797.
- Al-Widyan, M., Khasawneh, M., Abu-Dalo, M., 2021. Potential of floating photovoltaic technology and their effects on energy output, water quality and supply in Jordan. *Energies* 14, 1–13.
- Arpino, F., Cortellessa, G., Frattolillo, A., 2015. Experimental and numerical assessment of photovoltaic collectors performance dependence on frame size and installation technique. *Sol. Energy* 118, 7–19.
- Azmi, M.S.M., Othman, M.Y.H., Ruslan, M.H.H., Sopian, K., Majid, Z.A.A., 2013. Study on electrical power output of floating photovoltaic and conventional photovoltaic. *AIP Conf. Proc.* 1571, 95–101.
- Bontempo Scavo, F., Tina, G.M., Gagliano, A., Nizetić, S., 2021. An assessment study of evaporation rate models on a water basin with floating photovoltaic plants. *Int. J. Energy Res.* 45, 167–188.
- Cazzaniga, R., Cicu, M., Rosa-Clot, M., Rosa-Clot, P., Tina, G.M., Ventura, C., 2018. Floating photovoltaic plants: Performance analysis and design solutions. *Renew. Sustain. Energy Rev.* 81, 1730–1741.
- Choi, Y.K., 2014. A study on power generation analysis of floating PV system considering environmental impact. *Int. J. Softw. Eng. Its Appl.* 8, 75–84.
- Das, U.K., Tey, K.S., Seyedmahmoudian, M., Mekhilef, S., Idris, M.Y.I., Van Deventer, W., et al., 2018. Forecasting of photovoltaic power generation and model optimization: A review. *Renew. Sustain. Energy Rev.* 81, 912–928.
- Dörenkämper, M., Wahed, A., Kumar, A., de Jong, M., Kroon, J., Reindl, T., 2021. The cooling effect of floating PV in two different climate zones: A comparison of field test data from the Netherlands and Singapore. *Sol. Energy* 214, 239–247.
- Dubey, S., Sarvaiya, J.N., Seshadri, B., 2013. Temperature dependent photovoltaic (PV) efficiency and its effect on PV production in the world - A review. *Energy Proc.* 33, 311–321.
- El-Agouz, S.A., Zayed, M.E., Abo Ghazala, A.M., Elbar, A.R.A., Shahin, M., Zakaria, M.Y., Ismaeil, K.K., 2022. Solar thermal

- feed preheating techniques integrated with membrane distillation for seawater desalination applications: Recent advances, retrofitting performance improvement strategies, and future perspectives. *Process Saf. Environ. Protect.* 164, 595–612.
- El-Hadary, M.I., Senthilraja, S., Zayed, M.E., 2023. A hybrid system coupling spiral type solar photovoltaic thermal collector and electrocatalytic hydrogen production cell: Experimental investigation and numerical modeling. *Process Saf. Environ. Protect.* 170, 1101–1120.
- Friel, D., Karimirad, M., Whittaker, T., Doran, J., Howlin, E., 2019. A review of floating photovoltaic design concepts and installed variations. 4th International Conference on Offshore Renewable Energy. CORE2019 Proceedings, Glasgow. ASRANet Ltd. [https://pure.qub.ac.uk/en/publications/a-review-of-floating-photovoltaic-design-concepts-and-installed-variations\(bf7bdfdf-feb7-46b8-8a52-bc144c3996f8\).html](https://pure.qub.ac.uk/en/publications/a-review-of-floating-photovoltaic-design-concepts-and-installed-variations(bf7bdfdf-feb7-46b8-8a52-bc144c3996f8).html).
- Gholami, H., Khalilnejad, A., Gharehpetian, G.B., 2015. Electro-thermal performance and environmental effects of optimal photovoltaic-thermal system. *Energy Convers. Manag.* 95, 326–333.
- Grubišić-Čabo, F., Nizetić, S., Giuseppe Marco, T., 2016. Photovoltaic panels: a review of the cooling techniques. *Trans. FAMENA* 40, 63–74.
- Khelifa, A., Kabeel, A.E., Attia, M.E.H., Zayed, M.E., Abdelgaied, M., 2023. Numerical analysis of the heat transfer and fluid flow of a novel water-based hybrid photovoltaic-thermal solar collector integrated with flax fibers as natural porous materials. *Renew. Energy* 217, 119245.
- Kjeldstad, T., Lindholm, D., Marstein, E., Selj, J., 2021. Cooling of floating photovoltaics and the importance of water temperature. *Sol. Energy* 218, 544–551.
- Kumar, M., Kumar, A., 2019. Experimental validation of performance and degradation study of canal-top photovoltaic system. *Appl. Energy* 243, 102–118.
- Kumar, M., Kumar, A., 2020. Experimental characterization of the performance of different photovoltaic technologies on water bodies. *Prog. Photovoltaics Res. Appl.* 28, 25–48.
- Kumar, N.M., Subramaniam, U., Mathew, M., Ajitha, A., Almakhlles, D.J., 2020. Exergy analysis of thin-film solar PV module in ground-mount, floating and submerged installation methods. *Case Stud. Therm. Eng.* 21, 100686.
- Kumari, P.A., Geethanjali, P., 2018. Parameter estimation for photovoltaic system under normal and partial shading conditions: A survey. *Renew. Sustain. Energy Rev.* 84, 1–11.
- Liu, L., Wang, Q., Lin, H., Li, H., Sun, Q., Wennersten, R., 2017. Power Generation Efficiency and Prospects of Floating Photovoltaic Systems. *Energy Proc.* 105, 1136–1142.
- Liu, H., Krishna, V., Lun Leung, J., Reindl, T., Zhao, L., 2018. Field experience and performance analysis of floating PV technologies in the tropics. *Prog. Photovoltaics Res. Appl.* 26, 957–967.
- Mehrotra, S., Rawat, P., Debbarma, M., Sudhakar, K., Centre, E., Pradesh, M., 2014. Performance of a solar panel.pdf. *Int. J. Sci. Environ.* 3, 1161–1172.
- Mittal, D., Saxena, B.K., Rao, K.V.S., 2018. Comparison of floating photovoltaic plant with solar photovoltaic plant for energy generation at Jodhpur in India. *Proceedings of 2017 IEEE International Conference on Technological Advancements in Power and Energy: Exploring Energy Solutions for an Intelligent Power Grid, TAP Energy 2017*, pp. 1–6.
- Moharram, K.A., Abd-Elhady, M.S., Kandil, H.A., El-Sherif, H., 2013. Enhancing the performance of photovoltaic panels by water cooling. *Ain Shams Eng. J.* 4, 869–877.
- Ram, J.P., Babu, T.S., Rajasekar, N., 2017. A comprehensive review on solar PV maximum power point tracking techniques. *Renew. Sustain. Energy Rev.* 67, 826–847.
- Rosa-Clot, M., Tina, G.M., Nizetic, S., 2017. Floating photovoltaic plants and wastewater basins: An Australian project. *Energy Proc.* 134, 664–674.
- Sivakumar, B., Navakrishnan, S., Cibi, M.R., Senthil, R., 2021. Experimental study on the electrical performance of a solar photovoltaic panel by water immersion. *Environ. Sci. Pollut. Res.* 28, 42981–42989.
- Trapani, K., Millar, D.L., 2014. The thin film flexible floating PV (T3F-PV) array: The concept and development of the prototype. *Renew. Energy* 71, 43–50.
- Zhou, J., Yi, Q., Wang, Y., Ye, Z., 2015. Temperature distribution of photovoltaic module based on finite element simulation. *Sol. Energy* 111, 97–103.